Electronic Supplementary Material (ESI) for Chemical Communications.

Green-emitting dendritic alkynylgold(III) complexes with excellent film morphology for the applications in solution-processable organic light-emitting devices

Man-Chung Tang, Lianne Hei-Yin Lo, Wai-Lung Cheung, Shiu-Lun Lai, Mei-Yee Chan and Vivian Wing-Wah Yam**

[*] Dr. M.-C. Tang, Ms. L. H.-Y. Lo, Mr. W.-L. Cheung, Dr. S.-L. Lai, Dr. M.-Y. Chan* and Prof. Dr. V. W.-W. Yam*
Institute of Molecular Functional Materials [Areas of Excellence Scheme, University Grants Committee (Hong Kong)] and Department of Chemistry, The University of Hong Kong, Pokfulam Road, Hong Kong, P. R. China.
Fax: +(852) 2857 1586; Tel: +(852) 2859 2153
Email: wwyam@hku.hk; chanmym@hku.hk

Electronic Supplementary Information

Experimental Section

Experimental Sections

Materials and Reagents.

Tetra-*n*-butylammonium hexafluorophosphate (Aldrich, 98 %) was recrystallized more than three times from hot absolute ethanol before use. 4-((Triisopropylsilyl)ethynyl)aniline was synthesized according to literature procedure.[1] Toluene and tetraydrofuran (THF) for reactions were purified by the Innovative Technology, Inc. PureSolv MD 5 Solvent Purification System before use. Triethylamine was distilled over calcium hydride before use. All other reagents were of analytical grade and were used as received. All reactions were performed under anaerobic conditions using standard Schlenk techniques under nitrogen atmosphere unless specified otherwise.

Physical Measurements and Instrumentation.

Absportion, emission spectra and photoluminescence quantum yield (PLQY) measurements

The UV−visible absorption spectra were recorded on a Cary 60 UV−vis (Agilent Technology) spectrophotometer equipped with a xenon flash lamp. ^{1}H and ^{13}C{^{1}H} nuclear magnetic resonance (NMR) spectra were recorded on a Bruker Avance 400 (400 MHz for ^{1}H and 100 MHz for ^{13}C nuclei) or Bruker Avance 500 (500 MHz for ^{1}H and 125 MHz for ^{13}C nuclei) Fourier-transform NMR spectrometer with chemical shifts reported relative to tetramethylsilane (δ = 0 ppm) in chloroform or residual solvent peak(s) in dichloromethane (δ = 5.32 ppm), and THF (δ = 1.72 and 3.58 ppm). ^{19}F{^{1}H} NMR spectra were recorded on a Bruker Avance 400 (376 MHz for ^{19}F nucleus) or Bruker Avance 500 (470 MHz for ^{19}F nucleus) Fourier-transform NMR spectrometer. Positive high resolution-electrospray ionization mass spectrometry (HR-ESI-MS) spectra were recorded on Bruker MaXis II Quadrupole time-of-flight (QTOF) MS. IR spectra were recorded as KBr disks on a Bio-Rad FTS-7 FTIR spectrometer (4000−400 cm^{-1}). Elemental analyses of compounds were performed on a Carlo Erba 1106 elemental analyzer at the Institute of Chemistry, Chinese Academy of Sciences in Beijing. Steady-state excitation and emission spectra were recorded on a Spex Fluorolog-3 Model FL3-211 fluorescence spectrofluorometer equipped with a R2658P PMT detector or a Horiba Fluoromax-4 fluorescence spectrofluorometer equipped with a R928P PMT detector. Solid-state photophysical measurements were performed with solid sample loaded into a quartz tube inside a quartz-walled Dewar flask. Low-temperature (77 K) photophysical measurements were done by placing liquid nitrogen into the optical Dewar flask.

Excited-state lifetimes of solution, solid and glass samples were measured with a conventional laser system. The excitation source used was the 355 nm output (third harmonic, 8 ns) of a Spectra-Physics QuantaRay Q-switched GCR-150 pulsed Nd:YAG laser (10 Hz). Luminescence decay signals were recorded by a Hamamatsu R928 photomultiplier tube, recorded on a Tektronix model TDS-620A (500 MHz, 2 GS s^{-1}) digital oscilloscope and analyzed with a program for exponential fits, while the excited-state lifetimes of thin film samples were measured on a Hamamatsu C11367 Quantaurus-Tau Compact Fluorescence Lifetime Spectrometer. Relative PLQYs were measured by the optical dilute method reported by Demas and Crosby.[2] A degassed solution of $[Ru(bpy)_3]Cl_2$ in acetonitrile (Φ_{lum} = 0.06, excitation wavelength at 436 nm) was used as the reference,[2] whereas absolute PLQYs of thin films were measured on a Hamamatsu C9920-03G Absolute Photoluminescence Quantum Yield Measurement System. Cyclic voltammetry was performed with a CH Instruments Model CHI620E (CH Instruments, Inc.). All solutions for electrochemical measurements were purged with prepurified argon gas prior to measurement.

Thermogravimetric and atomic force microscopy (AFM) measurements.

Thermal analyses were performed with Q50 Thermogravimetric Analyzer (TA Instruments), in which the decomposition temperature, T_d, is defined as the temperature at which the sample shows a 5 % weight loss. AFM experiments were performed on an Asylum research MFP-3D Stand Alone Atomic Force Microscope in tapping mode under ambient conditions. The microscope was equipped with an All-Digital ARC2 Controller.

Device fabrication and characterization.

Solution-processable OLEDs were fabricated on patterned indium-tin-oxide (ITO) glass substrates with a sheet resistance of 30 Ω per square. The substrates were cleaned with Decon 90, rinsed with deionized water, dried in an oven, and finally treated in an ultraviolet-ozone chamber. A 40-nm thick poly(ethylenedioxythiophene):poly(styrene sulfonic acid) (PEDOT:PSS) layer was spin-coated onto the ITO coated glass substrates as hole-transporting layer. After that, the emissive layer was formed by mixing the gold(III) complex with *N*,*N*′-dicarbazolyl-3,5-benzene (MCP) to prepare a 10 mg cm^{-3} solution in chloroform and spin-coated onto the PEDOT:PSS layer to give uniform thin films of 30-nm thickness. Onto this, a 5-nm thick tris(2,4,6-trimethyl-3-(pyridin-3-yl)phenyl)borane (3TPYMB) and a 30-nm thick 1,3,5-tri[(3-pyridyl)phen-3-yl]benzene (TmPyPB)

were evaporated as a hole-blocking layer and an electron-transporting layer, respectively; while LiF/Al was used as the metal cathode. All organic and metal films were sequentially deposited at a rate of 0.1–0.2 nm s^{-1} without vacuum break. A shadow mask was used to define the cathode and to make four 0.1 cm^2 devices on each substrate. Current density–voltage–luminance characteristics and electroluminescence (EL) spectra were measured simultaneously with a programmable Keithley model 2400 power source and a Photoresearch PR-655 spectrometer under ambient conditions.

Synthesis and Characterization

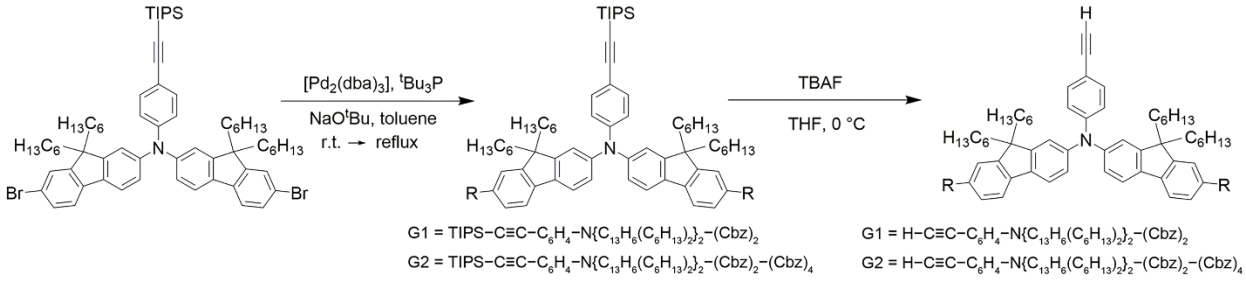

Scheme S1. Synthetic routes to alkynes

Synthesis of the alkynyls and their precursors

TIPS−C≡C−C_6H_4−N{$C_{13}H_6(C_6H_{13})_2$}$_2$−$(Cbz)_2$. This was prepared according to modification to a literature procedure for Buchwald-Hartwig amination.[1] A white solid was obtained. Yield: 500 mg, 86 %. ^{1}H NMR (500 MHz, chloroform-d_1, δ / ppm): δ 8.18 (d, J = 8.0 Hz, 4H), 7.84 (d, J = 8.0 Hz, 2H), 7.67 (d, J = 8.8 Hz, 2H), 7.48−7.56 (m, 4H), 7.36−7.47 (m, 10H), 7.27−7.34 (m, 4H), 7.24 (s, 2H), 7.12 (t, J = 8.8 Hz, 4H), 1.86−2.00 (m, 8H), 1.08−1.25 (m, 45H), 0.78−0.88 (m, 20H); ^{13}C{^{1}H} NMR (125 MHz, chloroform-d_1, δ / ppm): δ 152.73, 152.65, 148.20, 146.92, 141.25, 140.25, 136.18, 136.01, 133.24, 126.04, 126.02, 124.04, 123.51, 122.53, 121.89, 120.87, 120.52, 120.41, 119.99, 119.53, 116.90, 109.94, 107.38, 89.83, 55.59, 40.31, 31.77, 29.77, 24.16, 22.72, 18.88, 14.22, 11.54. HRMS (positive ESI) found 1268.8034 $[M+H]^+$; Calculated for $C_{91}H_{105}N_3Si$ (*m/z*) 1268.8072.

TIPS−C≡C−C_6H_4−N{$C_{13}H_6(C_6H_{13})_2$}$_2$−$(Cbz)_2$−$(Cbz)_4$. This was prepared according to modification to a literature procedure for Buchwald-Hartwig amination.[1] A pale yellow solid was

obtained. Yield: 1.06 g, 75 %. ^{1}H NMR (500 MHz, chloroform-d_1, δ / ppm): δ 8.32 (d, J = 1.2 Hz, 4H), 8.18 (td, J = 1.2 Hz, 8.0 Hz, 8H), 7.96 (d, J = 8.5 Hz, 2H), 7.60−7.77 (m, 14H), 7.35−7.48 (m, 18H), 7.26−7.33 (m, 10H), 7.10−7.21 (m, 4H), 1.93−2.13 (m, 8H), 1.10−1.32 (m, 45H), 0.72−1.00 (m, 20 H); ^{13}C{^{1}H} NMR (125 MHz, chloroform-d_1, δ / ppm): δ 153.07, 152.80, 148.10, 147.21, 141.99, 141.07, 135.94, 135.34, 133.31, 130.52, 126.43, 126.15, 126.06, 124.10, 123.36, 122.78, 121.91, 121.10, 120.75, 120.47, 119.98, 119.87, 119.53, 117.24, 111.43, 109.85, 107.28, 90.06, 55.77, 40.36, 31.80, 29.80, 24.25, 22.72, 18.85, 14.24, 11.55. HRMS (positive ESI) found 1928.0297 $[M+H]^+$; Calculated for $C_{139}H_{133}N_7Si$ (*m/z*) 1928.0386.

H−C≡C−C_6H_4−N{$C_{13}H_6(C_6H_{13})_2$}$_2$−$(Cbz)_2$. To the solution of TIPS−C≡C−C_6H_4−N{$C_{13}H_6(C_6H_{13})_2$}$_2$ −$(Cbz)_2$ (500 mg, 0.39 mmol) in THF was added TBAF (1.19 mL, 1.0 M in THF) dropwise at 0 °C. Upon completion of reaction, the mixture was concentrated. The mixture was then diluted with CH_2Cl_2 and water. The organic layer was extracted and washed with water twice, followed by brine. The organic layer was dried over anhydrous $MgSO_4$, filtered, and then concentrated. The product was purified by column chromatography on silica gel with hexane and dichloromethane (v/v = 5:1) as eluent to give an off-white solid after solvent removal. Yield: 225 mg, 51 % ^{1}H NMR (500 MHz, chloroform-d_1, δ / ppm): δ 8.17 (d, J = 8.0 Hz, 4H), 7.83 (d, J = 8.0 Hz, 2H), 7.67 (d, J = 8.0 Hz, 2H), 7.48−7.55 (m, 4H), 7.37−7.47 (m, 10H), 7.26−7.34 (m, 4H), 7.23 (s, 2H), 7.08−7.18 (m, 4H), 3.07 (s, 1H), 1.84−2.02 (m, 8H), 1.03−1.29 (m, 24H), 0.73−0.90 (m, 20H); ^{13}C{^{1}H} NMR (125 MHz, chloroform-d_1, δ / ppm): δ 152.77, 152.65, 148.65, 146.80, 141.24, 140.19, 136.35, 136.06, 133.31, 126.05, 124.22, 123.52, 122.21, 121.89, 120.92, 120.52, 120.45, 120.00, 119.73, 115.12, 109.93, 84.00, 76.59, 55.59, 40.31, 31.77, 29.78, 24.16, 22.74, 14.22. HRMS (positive ESI) found 1111.6716 $[M+H]^+$; Calculated for $C_{82}H_{85}N_3$ (*m/z*) 1111.6738.

H−C≡C−C_6H_4−N{$C_{13}H_6(C_6H_{13})_2$}$_2$−$(Cbz)_2$−$(Cbz)_4$. This was synthesized by a similar procedure as H−C≡C−C_6H_4−N{$C_{13}H_6(C_6H_{13})_2$}$_2$−$(Cbz)_2$ except that TIPS−C≡C−C_6H_4−N{$C_{13}H_6(C_6H_{13})_2$}$_2$−$(Cbz)_2$ was replaced with TIPS−C≡C−C_6H_4−N{$C_{13}H_6(C_6H_{13})_2$}$_2$−$(Cbz)_2$−$(Cbz)_4$ (1.06 g, 0.55 mmol). A pale yellow solid was obtained. Yield: 882 mg, 90 % ^{1}H NMR (500 MHz, chloroform-d_1, δ / ppm): δ 8.33 (d, J = 1.8 Hz, 4H), 8.19 (d, J = 7.8 Hz, 8H), 7.97 (d, J = 8.6 Hz, 2H), 7.77 (d, J = 8.2 Hz, 2H), 7.68−7.74 (m, 8H), 7.67 (dd, J = 1.8 Hz, 8.6 Hz, 4H), 7.38−7.49 (m, 18H), 7.26−7.35 (m, 10H), 7.22 (dd, J = 1.8 Hz, 8.2 Hz, 2H), 7.19 (d, J = 8.6 Hz, 2H), 3.12 (s, 1H), 1.96−2.13 (m, 8H), 1.12−1.30 (m, 24H), 0.79−0.99 (m, 20H); ^{13}C{^{1}H} NMR

(125 MHz, tetrahydrofuran-d_8, δ / ppm): δ 153.05, 152.80, 148.54, 147.07, 141.95, 141.02, 140.97, 136.08, 135.36, 133.37, 130.48, 126.41, 126.14, 126.05, 124.25, 124.08, 123.32, 122.48, 121.88, 121.14, 120.79, 120.47, 119.96, 119.86, 119.68, 115.43, 111.41, 109.84, 83.90, 76.76, 55.75, 40.35, 31.79, 29.80, 24.23, 22.71, 14.25. HRMS (positive ESI) found 1771.8997 $[M+H]^+$; Calculated for $C_{130}H_{113}N_7$ (*m/z*) 1771.9052.

Synthesis of Alkynylgold(III) Dendrimers

[Au((*p*-CF_3)–C^N(*p*-OMe)^C–(CF_3-*p*))[C≡C–C_6H_4–N{$C_{13}H_7(C_6H_{13})_2$}$_2$]] (**1**). This was synthesized according to modification of literature procedure for the related tridentate ligand-containing cyclometalated gold(III) alkynyl complexes.[3–4] A bright yellow solid was obtained. Yield: 110 mg, 40 %. ^{1}H NMR (500 MHz, tetrahydrofuran-d_8, δ / ppm): δ 8.26 (s, 2H, –pyridyl protons), 7.80 (d, *J* = 8.5 Hz, 2H, –$C_6H_3CF_3$– of C^N^C), 7.62–7.68(m, 4H, fluorenyl protons), 7.40–7.49 (m, 4H, –$C_6H_3CF_3$– of C^N^C and –C_6H_4–), 7.37 (s, 2H, –$C_6H_3CF_3$– of C^N^C), 7.33 (d, *J* = 7.5 Hz, 2H, fluorenyl protons), 7.24–7.31 (m, 4H, fluorenyl protons), 7.22 (td, *J* = 7.5 Hz, 1.5 Hz, 2H, fluorenyl protons), 7.11 (d, *J* = 9.0 Hz, 2H, –C_6H_4–), 7.07 (dd, *J* = 7.5 Hz, 1.5 Hz, 2H, fluorenyl protons), 4.11 (s, 3H, –OCH_3), 1.89–2.04 (m, 8H, hexyl protons), 1.05–1.23 (m, 24H, hexyl protons), 0.60–0.85 (m, 20H, hexyl protons); ^{13}C{^{1}H} NMR (125 MHz, tetrahydrofuran-d_8, δ / ppm): δ 171.74, 166.24, 164.71, 153.67, 153.04, 152.08, 150.51, 147.36, 147.00, 141.18, 136.90, 132.57, 126.79, 126.35, 125.75, 125.47, 123.66, 123.55, 122.61, 122.55, 120.47, 120.16, 119.23, 119.13, 115.78, 105.58, 89.62, 78.60, 56.52, 55.09, 40.29, 31.71, 29.78, 23.91, 22.57, 13.56; ^{19}F{^{1}H} NMR (376 MHz, tetrahydrofuran-d_8, δ / ppm): δ –63.52; HRMS (positive ESI) found: 1373.5807 $[M+H]^+$; Calculated for $AuC_{78}H_{81}N_2F_6$: 1373.5992. Elemental analyses: found (%): C: 67.97 N: 2.21 H: 6.05. Calculated for $AuC_{78}H_{81}N_2F_6$: C: 68.21 N: 2.04 H: 5.94. IR (KBr): 2146 cm^{-1} *ν*(C≡C).

[Au((*p*-CF_3)–C^N(*p*-OMe)^C–(CF_3-*p*))[C≡C–C_6H_4–N{$C_{13}H_6(C_6H_{13})_2$}$_2$–$(Cbz)_2$]] (**2**). This was synthesized according to modification of literature procedure for the related tridentate ligand-containing cyclometalated gold(III) alkynyl complexes. An amber-colored solid was obtained. Yield: 62 mg, 38 %. ^{1}H NMR (500 MHz, chloroform-d_1, δ / ppm): δ 8.24 (s, 2H, –pyridyl protons), 8.17 (d, *J* = 8.0 Hz, 4H, carbazolyl protons), 7.85 (d, *J* = 8.0 Hz, 2H, fluorenyl protons), 7.70 (d, *J* = 8.0 Hz, 2H, fluorenyl protons), 7.49–7.56 (m, 6H, fluorenyl ptotons and –$C_6H_3CF_3$– of C^N^C), 7.40–7.47 (m, 10H, carbazolyl protons and –C_6H_4–), 7.35–7.39 (d, *J* = 8.0 Hz, 2H, –C_6H_4–), 7.27–

7.33 (m, 6H, carbazolyl protons and –$C_6H_3CF_3$– of C^N^C), 7.16–7.24 (m, 4H fluorenyl protons), 6.93 (s, 2H, –$C_6H_3CF_3$– of C^N^C), 4.06 (s, 3H, –OCH_3), 1.88–2.02 (m, 8H, hexyl protons), 1.10–1.26 (m, 24H, hexyl protons), 0.77–0.92 (m, 20H, hexyl protons); $^{13}C\{^1H\}$ NMR (125 MHz, chloroform-d_1, δ / ppm): δ 171.09, 166.21, 164.81, 152.72, 152.62, 152.03, 147.36, 147.18, 141.25, 140.38, 135.95, 135.89, 133.10, 132.81, 132.56, 126.05, 126.00, 125.38, 124.92, 123.91, 123.79, 123.76, 123.49, 123.20, 123.04, 121.88, 120.87, 120.51, 120.37, 119.96, 119.73, 119.33, 109.97, 104.95, 101.04, 89.65, 56.70, 55.61, 40.39, 31.79, 29.80, 24.17, 22.71, 14.22; $^{19}F\{^1H\}$ NMR (470 MHz, dichloromethane-d_2, δ / ppm): δ –62.95; HRMS (positive ESI) found: 1702.7036 $[M+H]^+$; Calculated for $AuC_{102}H_{95}N_4F_6O$: 1702.7070. Elemental analyses: found (%): C: 71.72 N: 3.35 H: 5.69. Calculated for $AuC_{102}H_{95}N_4F_6O$: C: 71.90 N: 3.29 H: 5.62. IR (KBr): 2146 cm^{-1} ν(C≡C).

[Au((*p*-CF_3)–C^N(*p*-OMe)^C–(CF_3-*p*))[C≡C–C_6H_4–N{$C_{13}H_6(C_6H_{13})_2$}$_2$–$(Cbz)_2$–$(Cbz)_4$]] (**3**). This was synthesized according to modification of literature procedure for the related tridentate ligand-containing cyclometalated gold(III) alkynyl complexes. A bright yellow solid was obtained. Yield: 320 mg, 60 %. ^1H NMR (500 MHz, chloroform-d_1, δ / ppm): δ 8.31 (d, J = 2.0 Hz, 4H, carbazolyl protons), 8.10–8.19 (m, 10H, carbazolyl protons and –pyridyl protons), 7.93–7.98 (m, 2H, –C_6H_4–), 7.77 (d, J = 8.5 Hz, 2H, fluorenyl protons), 7.67–7.73 (m, 8H, carbazolyl protons, fluorenyl protons and –C_6H_4–), 7.64 (dd, J = 2.0 Hz, J = 8.5 Hz, 4H, carbazolyl protons), 7.54 (d, J = 8.5 Hz, 2H, –$C_6H_3CF_3$– of C^N^C), 7.33–7.45 (m, 18H, carbazolyl protons and fluorenyl protons), 7.21–7.32 (m, 16H, carbazolyl protons and fluorenyl protons –$C_6H_3CF_3$– of C^N^C), 6.81 (s, 2H, –$C_6H_3CF_3$– of C^N^C), 4.02 (s, 3H, –OCH_3), 1.95–2.15 (m, 8H, hexyl protons), 1.10–1.35 (m, 24H, hexyl protons), 0.75–1.05 (m, 20H, hexyl protons); $^{13}C\{^1H\}$ NMR (125 MHz, chloroform-d_1, δ / ppm): δ 171.01, 166.09, 164.50, 153.03, 152.81, 151.94, 147.44, 147.28, 141.97, 141.15, 141.08, 135.79, 135.28, 133.12, 132.89, 132.64, 132.58, 132.39, 132.14, 130.49, 126.42, 126.16, 126.06, 125.37, 124.94, 124.09, 124.00, 123.71, 123.68, 123.34, 123.23, 123.20, 121.92, 121.12, 120.73, 120.46, 120.05, 119.97, 119.87, 119.36, 111.44, 109.86, 105.10, 100.81, 90.05, 56.64, 55.80, 40.44, 31.82, 29.83, 24.26, 22.70, 14.24; $^{19}F\{^1H\}$ NMR (470 MHz, dichloromethane-d_2, δ / ppm): δ –63.19; HRMS (positive ESI) found: 2362.9408 $[M+H]^+$ Calculated for $AuC_{150}H_{123}N_8F_6O$: 2362.9384. Elemental analyses: found (%): C: 74.01 N: 4.74 H: 5.05. Calculated for $AuC_{150}H_{123}N_8F_6O{\cdot}CH_2Cl_2$: C: 74.04 N: 4.57 H: 5.14. IR (KBr): 2146 cm^{-1} ν(C≡C).

Figures and Tables

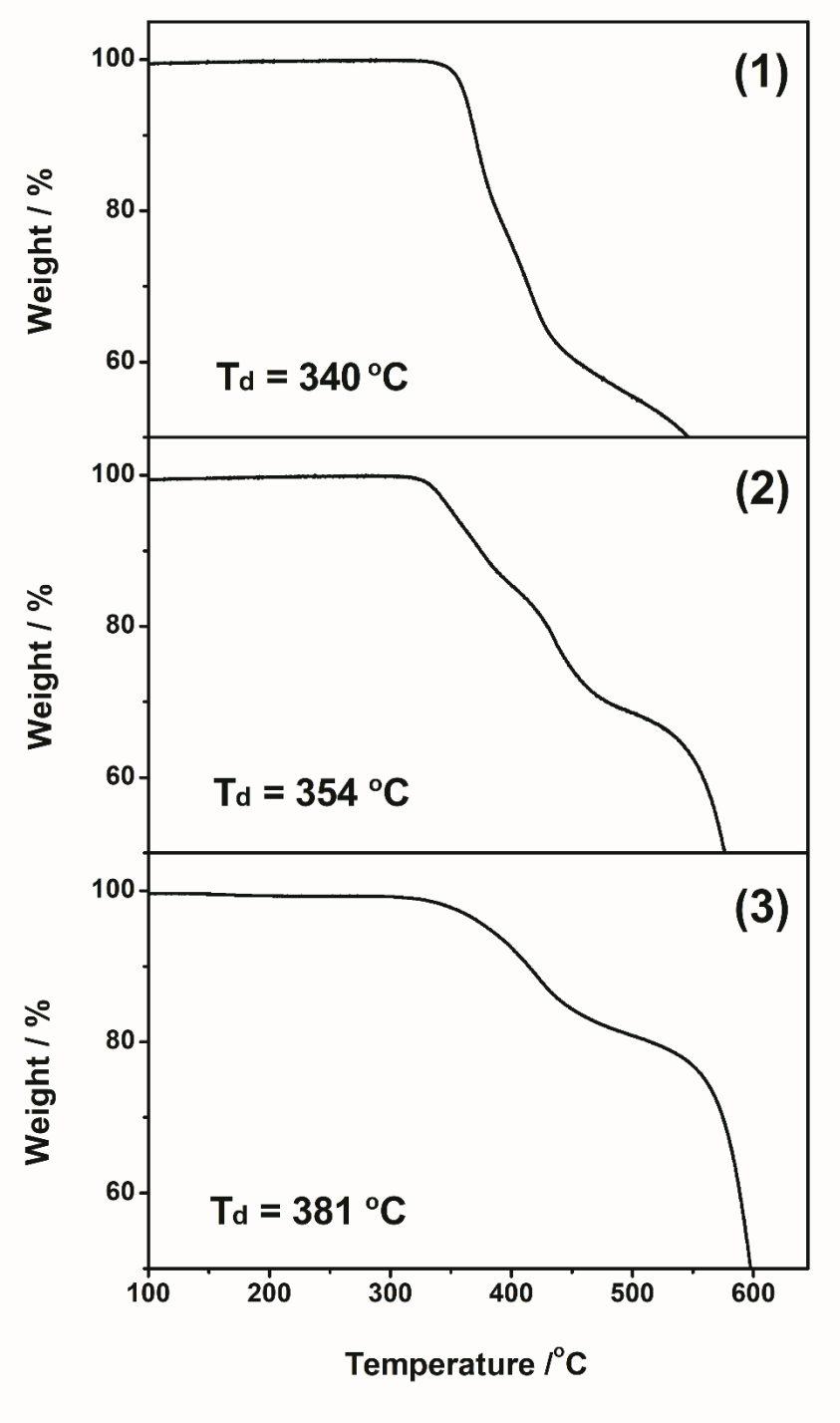

Figure S1. Thermogravimetric analysis (TGA) traces of **1**−**3**.

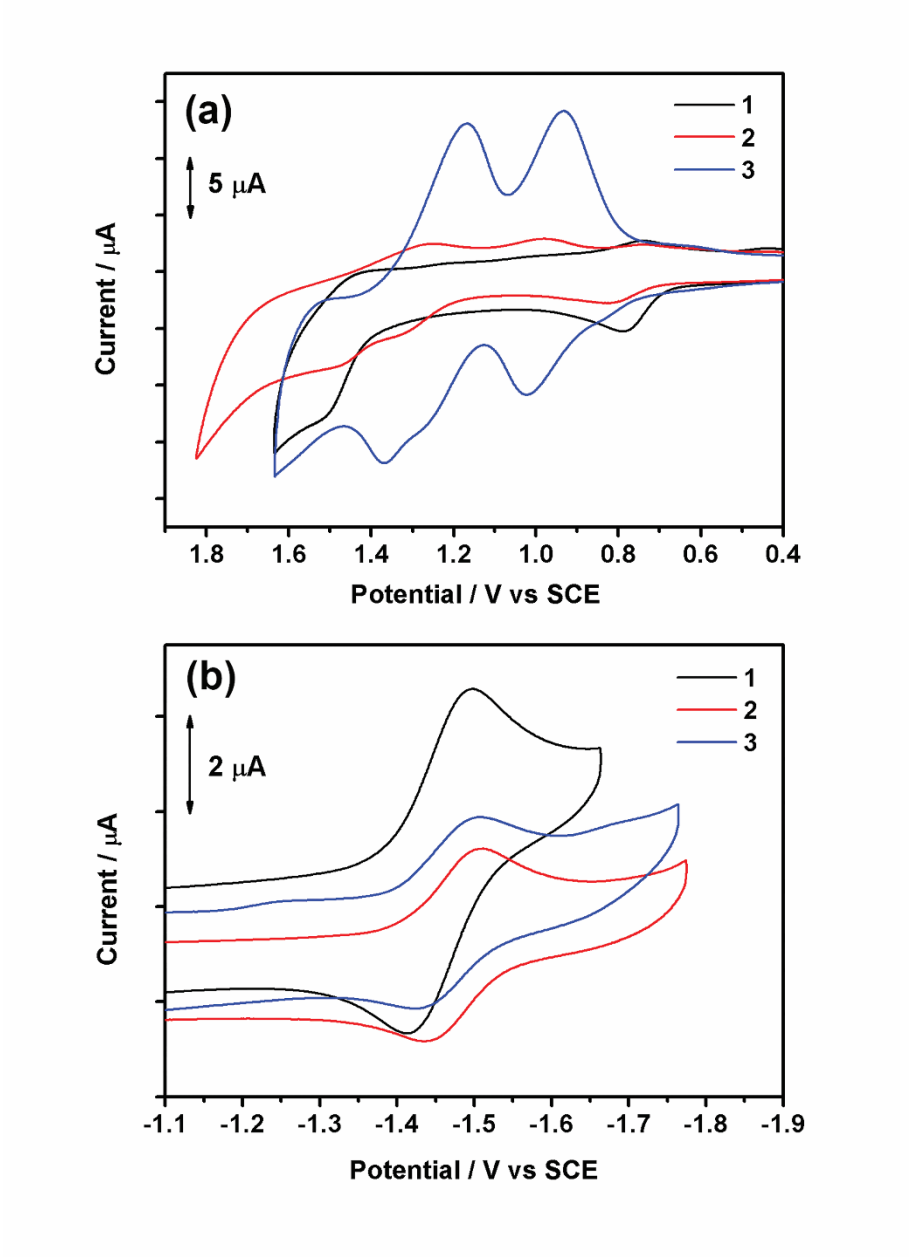

Figure S2. Cyclic voltammograms for the (a) oxidation and (b) reduction scans of **1**–**3** in degassed dichloromethane (0.1 M $^{n}Bu_4NPF_6$).

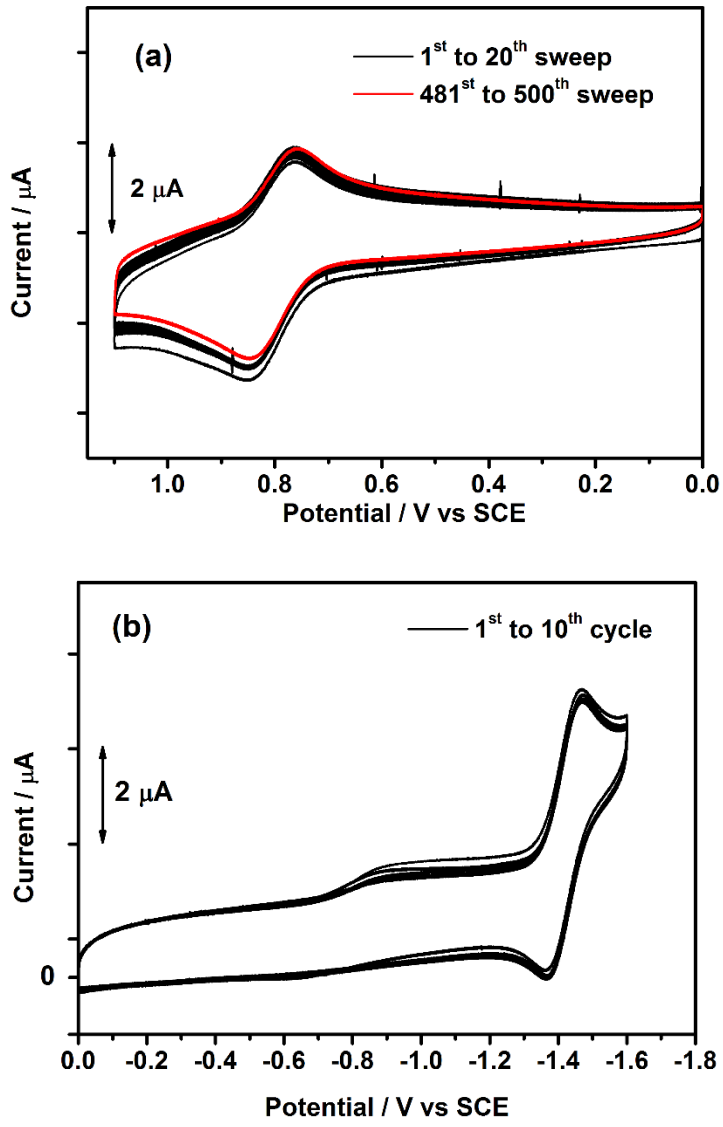

Figure S3. Cyclic voltammograms for the (a) oxidation scans after scanning of 500 cycles and (b) reduction scans after scanning of 10 cycles of **1** in degassed dichloromethane (0.1 M $^{n}Bu_4NPF_6$).

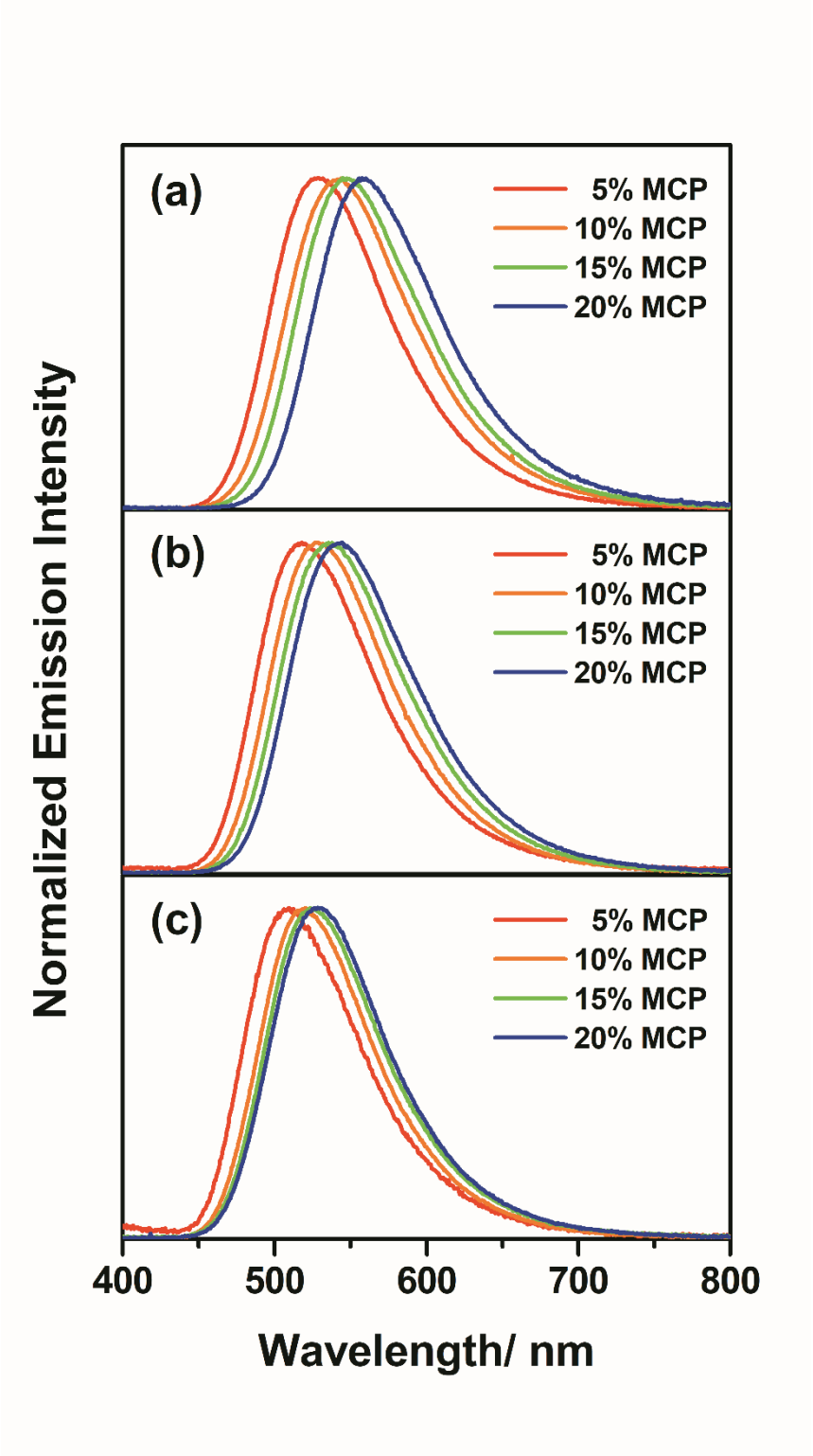

Figure S4. Concentration-dependent thin-film emission spectra of (a) **1**, (b) **2** and (c) **3** doped in MCP at 298 K.

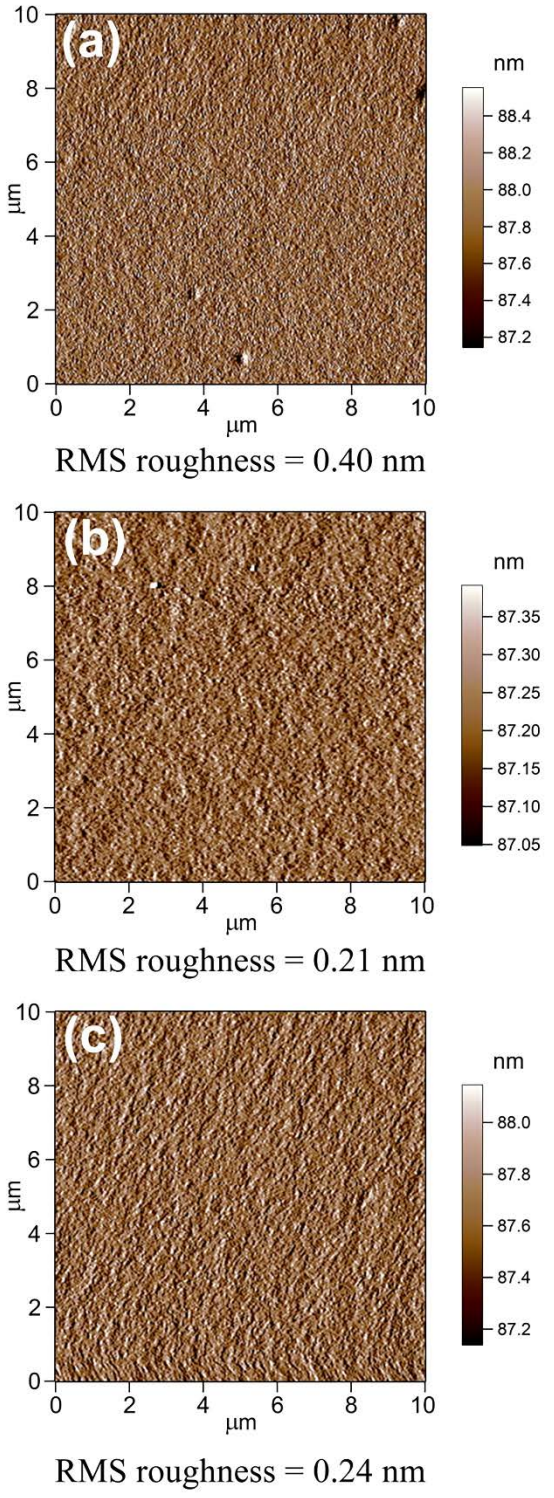

Figure S5. AFM images of (a) **1**, (b) **2** and (c) **3** films on ITO glass substrates.

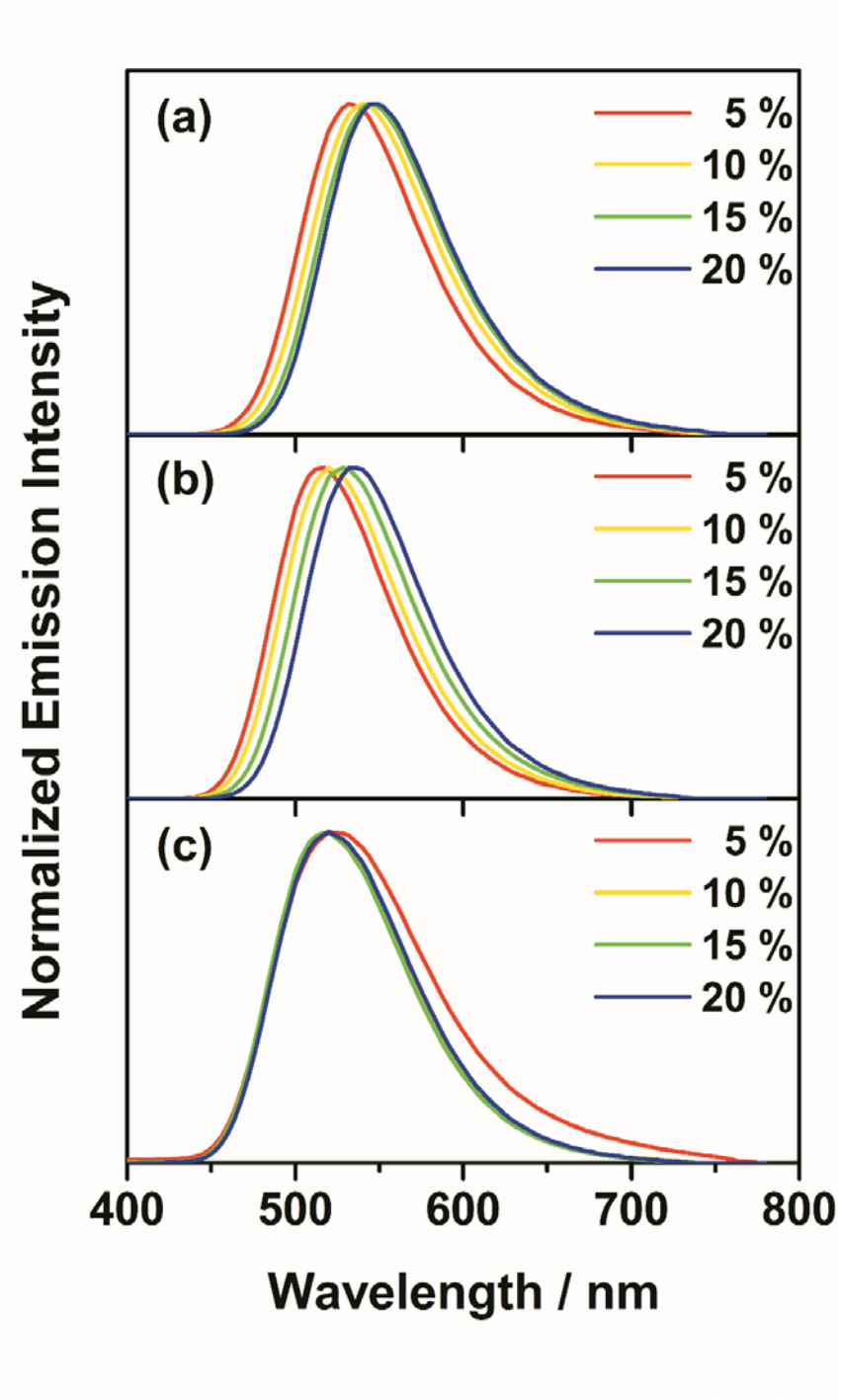

Figure S6. Normalized EL spectra of devices made with (a) **1**, (b) **2** and (c) **3** at different dopant concentrations.[5]

Table S1. Thermal properties of **1**–**3**.

Complex	T_d[a] / °C
1	340
2	354
3	381

[a] T_d is defined as the temperature at which the material showed a 5 % weight loss.

Table S2. Electrochemical data for **1**–**3**[a].

Complex	Oxidation [E_{pa} / V *vs* SCE][b] $E_{1/2}$ / V *vs* SCE[c] (E_p / mV)[d]	Reduction $E_{1/2}$ / V *vs* SCE[c] (E_p / mV)[d]	E_{HOMO} / eV[e]	E_{LUMO} / eV[e]
1	+0.76 (64), [+1.55]	–1.46 (90)	–5.56	–3.34
2	+0.77 (80), +1.29 (73), [+1.48]	–1.46 (75)	–5.57	–3.34
3	+0.81(78), +1.23(64), [+1.41]	–1.45 (80)	–5.61	–3.35

[a] In CH_2Cl_2 solution with 0.1 M $^nBu_4NPF_6$ as supporting electrolyte at 298 K. Working electrode; glassy carbon; scan rate = 100 mV s^{-1}.

[b] E_{pa} refers to the anodic peak potential for the irreversible oxidation wave.

[c] $E_{1/2} = (E_{pa} + E_{pc})/2$; E_{pa} and E_{pc} are the peak anodic and peak cathodic potentials, respectively.

[d] $E_p = (E_{pa} - E_{pc})$.

[e] E_{HOMO} and E_{LUMO} levels were calculated from electrochemical potentials, i.e. $E_{HOMO} = -e\ (4.8\ V + E_{pa})$; $E_{LUMO} = -e\ (4.8\ V + E_{pc})$.

Table S3. Photophysical properties of **1**–**3**.

Complex	Medium (T / K)	Absorption λ_{max} / nm (ε_{max} / $dm^3mol^{-1}cm^{-1}$)	Emission λ_{max} / nm (τ_o / μs)	Φ_{sol}[a]	Φ_{film}[b]
1	CH_2Cl_2 (298)	263 sh (78500), 305 sh (26000), 318 sh (33010), 362 (64770), 424 (10210)	693 (0.2)	0.01	
	Solid (298)		557 (0.2)		
	Solid (77)		553 (9.2)		
	Glass (77)[c]		491, 534 (454)		
	Thin film (298)				
	5 % in MCP		529 (4.6, 20.0)		0.85
	10 % in MCP		541 (2.3, 11.0)		0.87
	15 % in MCP		547 (1.5, 6.9)		0.87
	20 % in MCP		559 (1.4, 6.1)		0.83
2	CH_2Cl_2 (298)	293 (71200), 315 (47030), 357 sh (81845), 371 (59480), 423 (12850)	686 (0.2)	0.02	
	Solid (298)		581 (0.3)		
	Solid (77)		568 (12)		
	Glass (77)[c]		501, 542 (79)		
	Thin film (298)				
	5 % in MCP		517 (10.2, 55.0)		0.58
	10 % in MCP		530 (9.6, 52.7)		0.67
	15 % in MCP		535 (7.8, 38.6)		0.76
	20 % in MCP		542 (3.6, 27.4)		0.78
3	CH_2Cl_2 (298)	260 (225100), 293 (150190), 315 (74475), 342 sh (80900), 372 (89720), 422 sh (12675)	672 (0.2)	0.03	
	Solid (298)		579 (0.2)		
	Solid (77)		581 (5.0)		
	Glass (77)[c]		502, 545 (116)		
	Thin film (298)				
	5 % in MCP		508 (6.2, 37.6)		0.44
	10 % in MCP		520 (3.7, 21.2)		0.54
	15 % in MCP		523 (3.9, 18.7)		0.54
	20 % in MCP		528 (3.6, 15.1)		0.52

[a] The relative luminescence quantum yield in solution (Φ_{sol}) was measured at room temperature using degassed acetonitrile solution of $[Ru(bpy)_3]Cl_2$ as reference (excitation wavelength = 436 nm, Φ_{lum} = 0.06).

[b] Absolute luminescence quantum yield of thin film (Φ_{film}) of gold(III) compound doped into MCP thin film and was excited at wavelength of 320 nm.

[c] Measured in EtOH-MeOH-CH_2Cl_2 (40:10:1, v/v/v).

Table S4. Key characteristics of solution-processable OLEDs based on **1**–**3**.

Complex	Dopant concentration / wt%	Max. current efficiency / cd A^{-1}	Max. power efficiency / lm W^{-1}	Max. EQE / %	λ_{max} (FWHM) / nm (nm)[a]	CIE (x,y) [a]
1	5	28.3	8.6	8.2	532 (85)	0.34,0.59
	10	30.7	12.7	8.9	540 (85)	0.37,0.58
	15	41.0	24.2	11.8	544 (88)	0.39,0.58
	20	42.4	25.3	12.3	548 (87)	0.40,0.57
2	5	23.8	9.1	7.4	516 (81)	0.27,0.57
	10	26.3	10.4	8.0	520 (80)	0.29,0.58
	15	35.3	20.0	10.3	528 (83)	0.32,0.59
	20	51.1	37.7	14.5	536 (82)	0.35,0.59
3	5	22.5	17.7	7.4	520 (106)	0.32,0.54
	10	36.1	28.	11.8	520 (93)	0.29,0.55
	15	38.3	30.1	12.4	520 (92)	0.29,0.55
	20	36.4	28.6	11.5	520 (93)	0.30,0.56

[a] λ_{max} and CIE coordinates in parentheses, measured at 100 cd m^{-2}.

Computational Studies and Details

Density functional theory (DFT) calculations have been performed to gain further insight into the frontier molecular orbitals of complexes **1**−**3**. All calculations were carried out with the Gaussian 09 program suite.[6] The ground-state (S0) geometries of the model complexes of **1**−**3**, in which all the hexyl groups were replaced by methyl groups (labelled as complexes **1′**−**3′**) were fully optimized in toluene by DFT with the hybrid Perdew, Burke, and Ernzerhof (PBE0) functional,[7] in conjunction with the conductor-like polarizable continuum model (CPCM).[8] Vibrational frequency calculations were then performed on all stationary points to verify that each was a minimum (NIMAG = 0) on the potential energy surface. For all the calculations, the Stuttgart effective core potentials (ECPs) and the associated basis set were utilized to describe Au[9] with f-type polarization functions (ζ = 1.050),[10] whereas the 6-31G(d,p) basis set[11] was applied for all other atoms. All DFT and TDDFT calculations were performed with a pruned (99,590) grid for numerical integration. The selected frontier molecular orbitals of **1′**−**3′** are shown in Figures S6−S8, and the orbital energy diagram of the frontier molecular orbitals of **1′**−**3′** is shown in Figure S9. Upon going from **1′** to **3′**, the HOMO−LUMO energy gap increases from 2.76 to 2.87 eV, as the HOMO is destabilized from −4.97 to −5.15 eV with increasing dendrimer generations. Meanwhile, the energy of the LUMO localized on the C^N^C ligand is less perturbed by the substitution on the dendrimer. This trend is in line with that observed in the cyclic voltammograms, which show more positive potentials for oxidation and a similar reduction potential upon going from **1** to **3**.

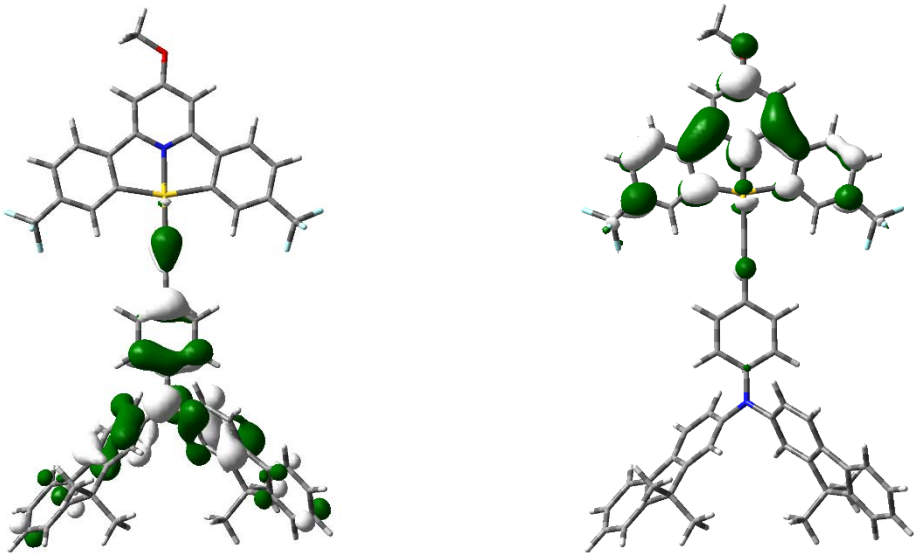

HOMO LUMO

Figure S6. Spatial plots (isovalue = 0.03) of selected frontier molecular orbitals of **1′** obtained from the PBE0/CPCM calculation.

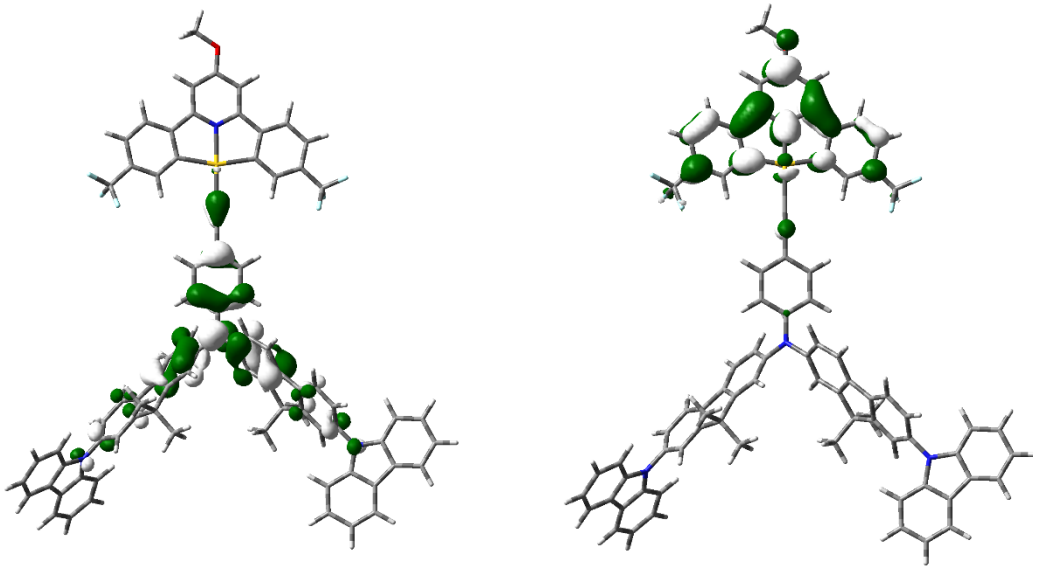

HOMO LUMO

Figure S7. Spatial plots (isovalue = 0.03) of selected frontier molecular orbitals of **2′** obtained from the PBE0/CPCM calculation.

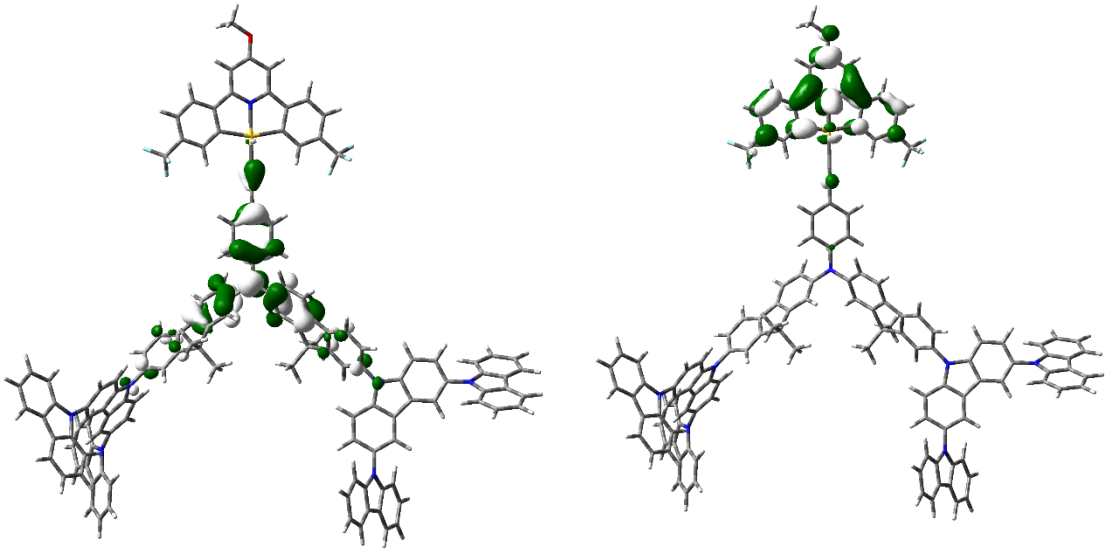

HOMO LUMO

Figure S8. Spatial plots (isovalue = 0.03) of selected frontier molecular orbitals of ***3′*** obtained from the PBE0/CPCM calculation.

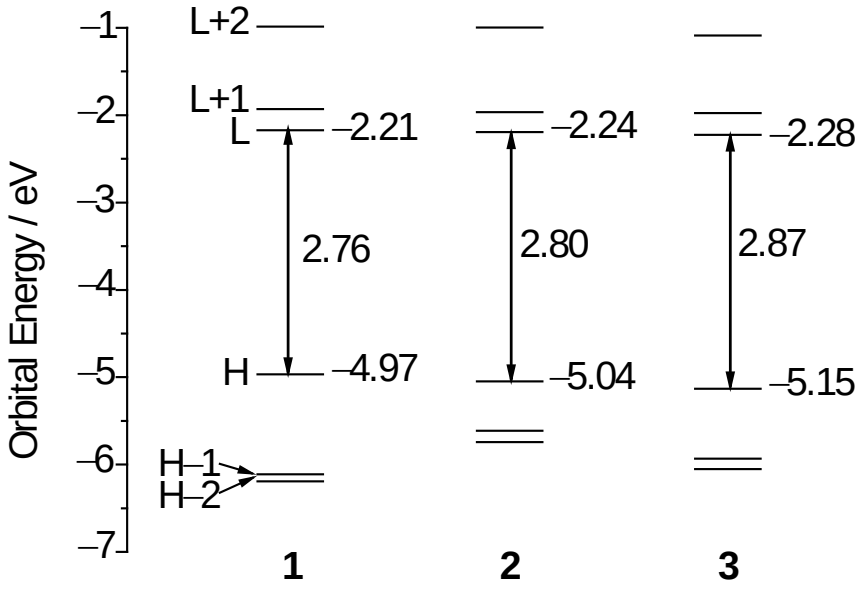

Figure S9. Orbital energy diagram of the frontier molecular orbitals (H = HOMO and L = LUMO) of **1′**–**3′**.

Acknowledgements

V.W.-W.Y. acknowledges UGC funding administrated by The University of Hong Kong (HKU) for supporting the Electrospray Ionization Quadrupole Time-of-Flight Mass Spectrometry Facilities under the Support for Interdisciplinary Research in Chemical Science, the HKU Development Fund and the Dr. Hui Wai Haan Fund for funding the X-Ray Diffractometer Facilities, and the support from HKU University Research Committee (URC) Strategically Oriented Research Theme on Functional Materials for Molecular Electronics Towards Materials and Energy Applications. The work described in this paper was fully supported by a grant from the University Grants Committee Areas of Excellence (AoE) Scheme from the Hong Kong Special Administrative Region, China (Project No. AoE/P-03/08). L.H.-Y.L. acknowledges the receipt of postgraduate studentships from HKU. The computations were performed using the HKU ITS research computing facilities. W.-K. K. and Dr. H.-L. A.-Y. are acknowledged for their assistance in the preparation of precursor gold(III) complexes and HR-ESI mass spectrometry characterization of compounds respectively. Dr. C. H. L. is acknowledged for his assistance in atomic force microscopy and the discussion of this manuscript.

References

1. C.-H. Lee, M.-C. Tang, Y.-C. Wong, M.-Y. Chan and V. W.-W. Yam, *J. Am. Chem. Soc.*, 2017, **139**, 10539–10550.
2. G. A. Crosby and J. N. Demas, *J. Phys. Chem.*, 1971, **75**, 991–1024.
3. M.-C. Tang, D. P.-K. Tsang, M. M.-Y. Chan, K. M.-C. Wong and V. W.-W. Yam, *Angew. Chem. Int. Ed.*, 2013, **125**, 464–467.
4. M.-C. Tang, C. K.-M. Chan, D. P.-K. Tsang, Y.-C. Wong, M. M.-Y. Chan, K. M.-C. Wong and V. W.-W. Yam, *Chem. Eur. J.*, 2014, **20**, 15233–15241.

5 A reduced bathochromic shift is observed for devices based on higher dendrimer generation. Particularly, devices made with **1** show a red shift in energy from 532 nm to 548 nm from 5 wt% to 20 wt%. On the other hand, the emission maximum remains unchanged at 520 nm for devices doped with **3**, even when the dopant concentration increases up to 20 wt%. Only a small emission broadening at *ca.* 600 nm was observed for the device doped with 5 wt% **3**, which may be attributed to the poor film quality that leads to inhomogeneity of the thin film that slightly broadens the emission band.

6 M. J. Frisch, G. W.Trucks, H. B. Schlegel, G. E. Scuseria, M. A. Robb, J. R. Cheeseman, G. Scalmani, V. Barone, B. Mennucci, G. A. Petersson, H. Nakatsuji, M. Caricato, X. Li, H. P. Hratchian, A. F. Izmaylov, J. Bloino, G. Zheng, J. L. Sonnenberg, M. Hada, M. Ehara, K. Toyota, R. Fukuda, J. IHasegawa, M. shida, T. Nakajima, Y. Honda, O. Kitao, H. Nakai, T. Vreven, J., J. A. Montgomery, J. E. Peralta, F. Ogliaro, M. Bearpark, J. J. Heyd, E. Brothers, K. N. Kudin, V. N. Staroverov, T. Keith, R. Kobayashi, J. Normand, K. Raghavachari, A.,Rendell, J. C. Burant, S. S. Iyengar, J. Tomasi, M. Cossi, N. Rega, J. M. Millam, M. Klene, J. E. Knox, J. B. Cross, V. Bakken, C. Adamo, J. Jaramillo, R. Gomperts, R. E. Stratmann, O. Yazyev, A. J. Austin, R. Cammi, C. Pomelli, J. W. Ochterski, R. L. Martin, K. Morokuma, V. G. Zakrzewski, G. A. Voth, P. Salvador, J. J. Dannenberg, S. Dapprich, A. D. Daniels, O. Farkas, J. B. Foresman, J. V. Ortiz, J. Cioslowski, D. J. Fox, *Gaussian 09 (Revision D.01)*, Gaussian, Inc.: Wallingford CT, 2013.

7 (a) J. P. Perdew, K. Burke, M. Ernzerhof, *Phys. Rev. Lett.* **1996**, *77*, 3865; (b) J. P. Perdew, K. Burke, M. Ernzerhof, *Phys. Rev. Lett.* **1997**, *78*, 1396; (c) C. Adamo, V. *J.* Barone, *Chem. Phys.* **1999**, *110*, 6158.

8 (a) V. Barone, M. Cossi, *J. Phys. Chem. A* **1998**, *102*, 1995; (b) M. Cossi, N. Rega, G. Scalmani, V. *J.* Barone, *Comput. Chem.* **2003**, *24*, 669.

9 D. Andrae, U. Haussermann, M. Dolg, H. Stoll, H. Preuss, *Theor. Chim. Acta.* **1990**, *77*, 123.

10 A. W. Ehlers, M. Böhme, S. Dapprich, A. Gobbi, A. Höllwarth, V. Jonas, K. F. Köhler, R. Stegmann, A. Veldkamp, G. Frenking, *Chem. Phys. Lett.* **1993**, *208*, 111.

11 W. J. Hehre, R. Ditchfie, J. A. Pople, *J. Chem. Phys.* **1972**, *56,* 2257; (b) P. C. Hariharan, J. A. Pople, *Theor. Chim. Acta.* **1973**, *28*, 213; (c) M. M. Francl, W. J. Pietro, W. J. Hehre, J. S. Binkley, M. S. Gordon, D. J. Defrees, J. A. Pople, *J. Chem. Phys.* **1982**, *77*, 3654.